THE PROBLEM OF NEGATIVE INDUCED POLARIZATION ANOMALIES

by

John S. Sumner

University of Arizona
Tucson, Arizona

NGR-03-002-091

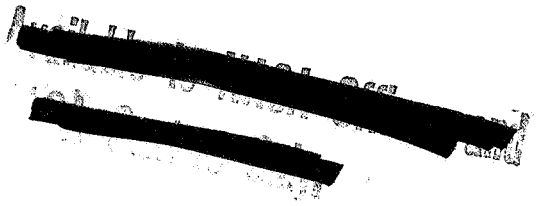

Presented at the Symposium on Induced Polarization
University of California
Berkeley, California
February 18 - 19, 1967

THE PROBLEM OF NEGATIVE INDUCED POLARIZATION ANOMALIES

Introduction

Negative IP anomalies have been observed by practically everyone that has made field measurements. In the earlier days of IP experimentation, some geophysicists doubted their real existance, while others ascribed these effects (and sometimes rightly so) to electromagnetic coupling or equipment problems. At least one person has theorized that some earth materials have negative IP properties by which these substances can be identified.

Negative anomalies have often been noted in drill hole, underground, and near surface mineralized areas. The magnitude of negative effects can be every bit as large as normal, positive effects. They are found with both frequency and time domain methods, using any given electrode array. They have confounded the interpretation of some otherwise successful surveys, and have sometimes created unnecessary confusion in taking field measurements.

It is the purpose of this report to discuss cause and characteristics of the negative IP effect. One should have an appreciation of this phenomenon if the subject of induced electrical polarization as a whole is to be understood. The negative effect is not actually a property of rocks but is due to an interaction of the geometry of polarizable bodies and measuring electrode positions.

Discussion

An illustration of positive and a negative IP decay waveforms in the time domain is shown on Figure 1. Both such curves can be readily observed in the laboratory, using real polarizable materials in an

electrolytic tank. The constant level charging current can be monitored as shown. Caution must be observed not to exceed realistic current densities in such laboratory experiments. Field measurements can also be devised near polarizable bodies to obtain comparable results.

Possible types of decay waveforms are shown next in Figure 2. If one will agree that it is indeed possible to have a negative IP waveform then it must be admitted that in some field circumstances positive and negative curves will possibly combine. Such combination will either result in cancellation of the IP effect, or produce composite curves as shown. Time constants of the positive and negative parts of the composite curve may be quite different, contributing to this peculiar wave form.

In order to better understand the electrical parameters that effect the induced electrical polarization of a material, let us review the response of a simple equivalent circuit. The circuit in Figure 3 is not intended to exactly reproduce a real IP response, but it will give results that are similar to rock polarization. A polarization resistance R_p in series with a capacitor C represents the blocking potential of metallic mineral particles. R_{DC} is the lower resistance of unblocked pore paths. Note that the capacitor can act like a switch which is essentially open at low frequencies and closed at high frequencies. The circuit can then be analysed to indicate that frequency effect is approximately equal to R_{DC} divided by R_p.

In the time domain, the same simplified circuit can be examined as shown in Figure 4. Chargeability M is defined as the area under the decay curve, normalized by dividing by the charging voltage V_o.

This is analytically equivalent to the product of R_{DC} and C. At any time t after the charging current is shut off, the decay voltage V_t is given by $Vo \left[\frac{R_{DC}}{R_{DC} + R_P}\right] e^{-t/\tau}$. Note that the time constant τ of the decay curve, which is defined as the time for the voltage to drop to $\frac{1}{e}$ or 63 percent of its initial value, is given by $(R_P + R_{DC})C$.

In the equivalent network the time constant of IP decay is dependent on circuit resistance. In rocks the decay constant is thus partly affected by resistivity, and other factors being equal conductive rocks should exhibit shorter decay constants. This fact can also be related to the metal factor parameter, or its time domain counterpart, static capacity. The metal factor is a normalization of the frequency effect, brought about by dividing by resistivity.

Induced electrical polarization in rocks seems to be principally caused by two similar electrochemical mechanisms, usually termed membrane polarization and electrode polarization. The ion cloud shown about the charged layered minerals in the upper diagram of Figure 5 drifts under the influence of an electrical field, giving rise to weak polarization effects on returning to equilibrium. A metallic mineral particle blocking a pore path has ions piling up against it in the lower diagram, creating a larger IP decay voltage at the cessation of current flow. The so-called solvated electron in pore electrolyte solution may play an important role in the polarization process. These polarization mechanisms do not in themselves suggest a possible negative phenomenon. Moreover, it is difficult to suggest any natural, physically reasonable mechanism or circuit which would exhibit a negative polarization effect.

Induced Electrical Polarization of a Sphere

The problem of a spherical conductor in a plane wave electric field has been studied by many investigators in the past, and implications of this situation are important to people doing resistivity and IP research. Figure 6 is a diagram plotted from results of measurements in the Geophysics Laboratory at the University of Arizona, showing current and potential lines near a conductive sphere. These results are similar to those of an equipotential survey over a conductive hemispherical body, using the gradient electrode array between distant, parallel line electrodes. Equipotential contour lines are solid, while orthogonal current flow lines are dashed in. The electric field within the sphere is seen to be uniform, in accordance with theory as originally developed by Gauss and more recently by Stratton (1941).

Figure 7 is a diagram first drawn by J. C. Maxwell (1873) who called it "lines of force and equipotential surfaces in a dimetral section of a spherical surface in which the superficial density is a harmonic of the first degree". This is the field of a polarized sphere, which of course has interesting geophysical applications in magnetism, gravity, and electrical exploration methods. Within the sphere equipotential surfaces have equidistant planes and the current density (although this may not be initially apparent) is constant. Exterior to the sphere the electric field is identical to that of a dipole, and is given by

$$\vec{E_t} = \frac{P}{r3}\left[2\vec{R}\,\mathrm{Cos}\Theta + \vec{\Theta}\,\mathrm{Sin}\,\Theta\right] \qquad (1)$$

Where P is the dipole moment, r the radius of the sphere, $\vec{R}$ and $\vec{\Theta}$ unit vectors in radial and tangential directions, and Θ is the polar angle.

The same data given on Figure 6 can be processed to show the gradient of the horizontal component at the electric field, as is plotted in Figure 8. This is an apparent resistivity diagram of a sphere in a plane wave field, and outside the sphere the contours show the horizontal component of a dipolar field. The originally uniform, parallel field can be represented by the potential gradient

$$\frac{\partial V}{\partial x} = \rho_o J \qquad (2)$$

where V is potential, J is current density, and ρ_o is background resistivity.

Potential and field exterior to the sphere can be calculated by combining the field of a dipole centered in the sphere with that of the parallel field. The potential outside the sphere where $(x^2+y^2)^{1/2} > r$ is

$$V = -P \frac{\rho_o J x}{(x^2+y^2)^{3/2}} \qquad (3)$$

and is indicated in Figure 6. The field in the x direction, which is proportional to apparent resistivity ρ_a, is

$$\frac{\partial V}{\partial x} = P \frac{\rho_o J (2x^2-y^2)}{(x^2+y^2)^{5/2}} \qquad (4)$$

In Figure 8, note the large apparent resistivity high zones off the ends of the body, which are related to the stronger potential gradients in the same region shown in Figure 6.

Surface resistivity measurements over a buried low resistivity sphere would see only the apparent resistivity low to be sensed over the equatorial region of this body. Diagrams of this sort have been

approximately calculated by Van Nostrand (1953) and Seigel (1959). The apparent resistivity within the sphere is indicated to be about twice that of the materials true resistivity; this is an example of the saturation effect.

The IP pattern shown in Figure 9 was made from laboratory results using the IP analog technique. It is also dipolar, being the algebraic difference between two dipolar fields, i.e. $(FE)_a = \frac{(\rho_a)_{HI} - (\rho_a)_{LO}}{(\rho_a)_{LO}}$ where $(FE)_a$ is apparent frequency effect and $(\rho_a)_{HI}$ and $(\rho_a)_{LO}$ are the apparent resistivities using high and low resistivity spheres. The IP modeling method is based on the finite difference approximation of the mathematical formulation originally developed by Seigel (1959) and Hallof (1964). It can be written that

$$(FE)_a = (FE)_1 \frac{\rho_1}{\rho_a} \frac{\partial \rho_a}{\partial \rho_1} \qquad (5)$$

where $(FE)_1$ and ρ_1 are the true frequency effect and true resistivity of the modeled polarizable sphere. Thus if one measures apparent resistivity of two contrasting bodies of identical geometry, an analog IP diagram can be made from the two sets of data. This is the basis for the laboratory analog model IP method.

The IP field in the spheres polar direction should theoretically be twice that in the equatorial plane, at a given distance, from equations (1) and (4). The measured analog IP values do not show this too well because of the finite interval of the gradient field measurement, and the inverse cube distance dependence. Nevertheless, the magnitude of the negative IP values is large as compared to the positive. These strong negatives are not often seen in surface surveys

because of the frequent presence of nonpolarizing near surface materials.

The final diagram, Figure 10, shows the nature of the instaneous IP field of a sphere after the polarizing current has been shut off. Charge has effectively accumulated at the interfacial boundary of the sphere, and this current would take an exact dipolar path if there were no resistivity contrast between sphere and matrix. The negative IP effect is simply a resultant of the vectorially negative horizontal component, from the sense of the charging current, as shown in the lower circle in Figure 10. If the polarizable sphere is conductive then the decay time constant will be affected, becoming an apparent time constant, which can contribute to the behavior of the composite curve.

Conclusions

This report has discussed the negative IP phenomenon and has presented an explanation of this problem, using the model of a polarized sphere. It is seen that negative effects can be quite large.

Composite waveforms can exist if positive and negative decays with different time constants combine algebraically. Interpretation of IP decay curve data should therefore be influenced by knowledge that composite effects will sometimes be seen in field results.

References

Hallof, P. G., 1964, A comparison of the various parameters employed in the variable frequency induced polarization method: Geophysics, v. 29, p. 425-433.

Maxwell, J. C., 1873, reprinted in 1954, A treatise on electricity and magnetism: New York, Dover Publications, Inc.

Seigel, H. O., 1959, Mathematical formulation and type curves for induced polarization: Geophysics, v. 24, p. 547-563.

Stratton, J. A., 1941, Electromagnetic theory: New York, McGraw-Hill Book Co., Inc.

Van Nostrand, R. G., 1953, Limitations on resistivity methods as inferred from the buried sphere problem: Geophysics, v. 18, p. 423-433.

List of Figures

PULSE DECAY WAVEFORMS

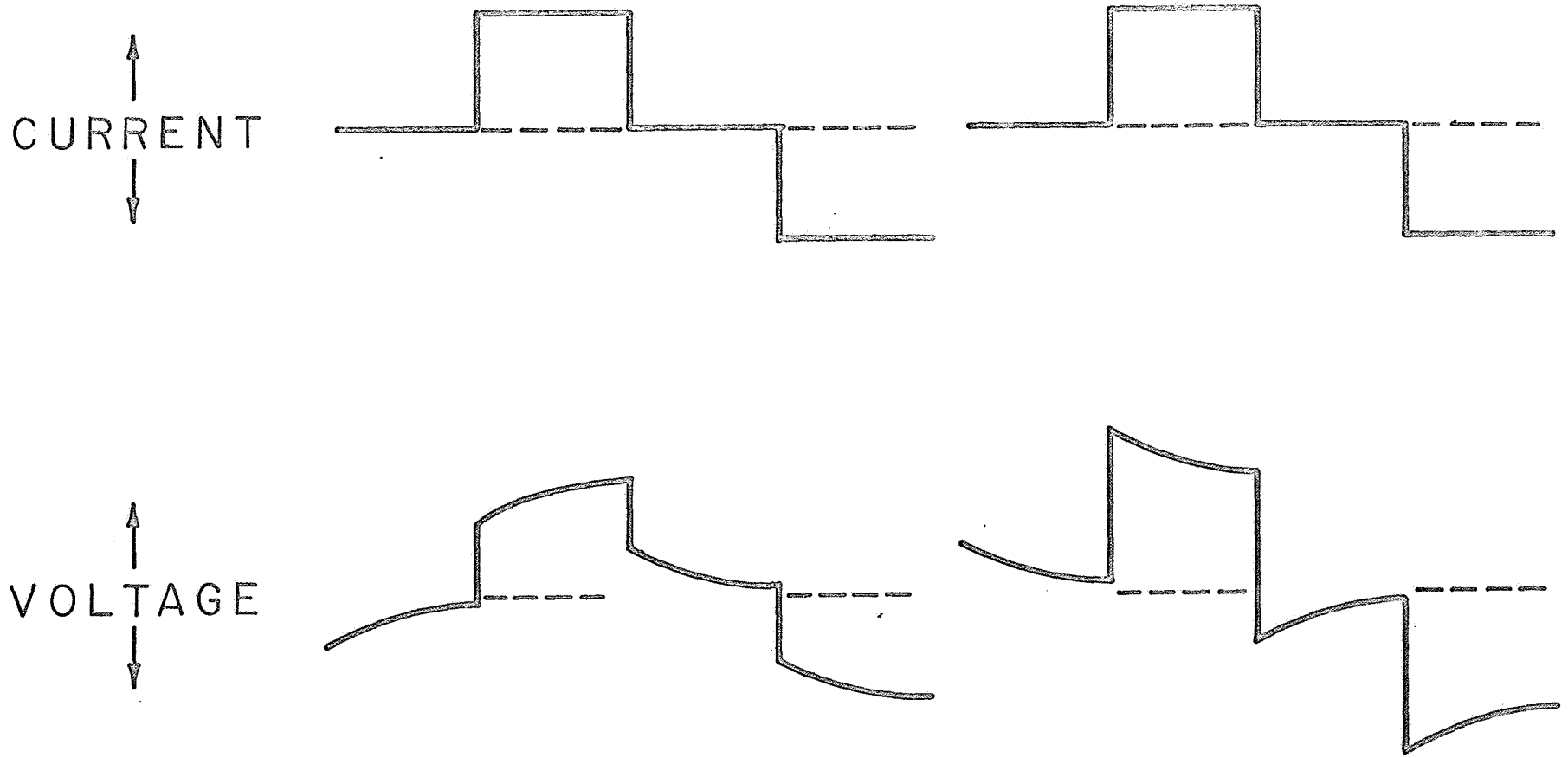

TYPES OF DECAY WAVEFORMS

CURRENT

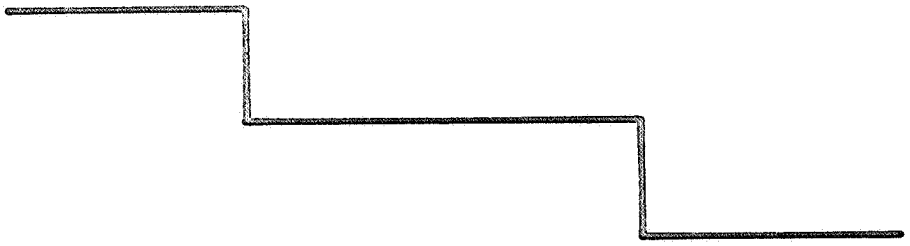

NORMAL

NEGATIVE

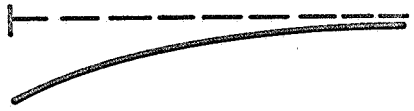

COMPOSITE I

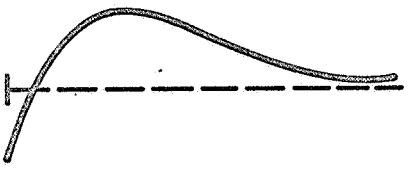

COMPOSITE II

EQUIVALENT CIRCUIT

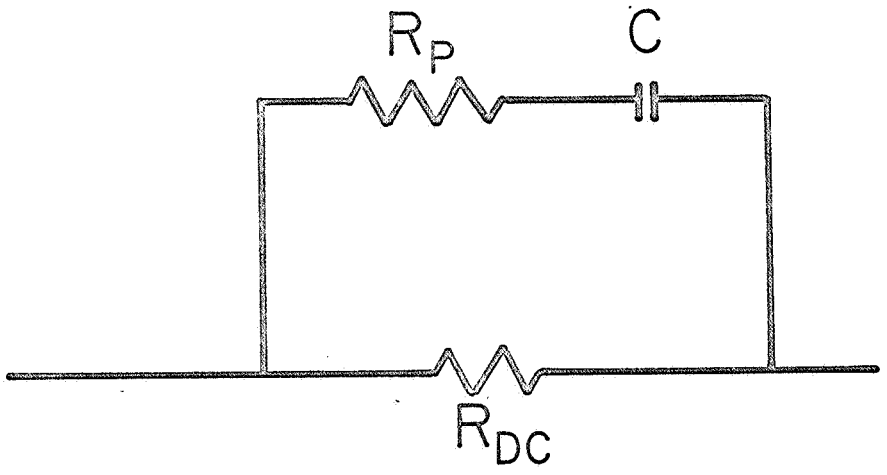

LOW FREQ. VOLTS: $V_{Lo} = R_{DC}$

HIGH FREQ. VOLTS: $V_{Hi} = \frac{R_P R_{DC}}{R_P + R_{DC}}$

FREQUENCY EFFECT: $FE = \frac{V_{Lo} - V_{Hi}}{V_{Hi}}$

$= \frac{R_{DC}}{R_P}$

CIRCUIT ANALYSIS
TIME DOMAIN

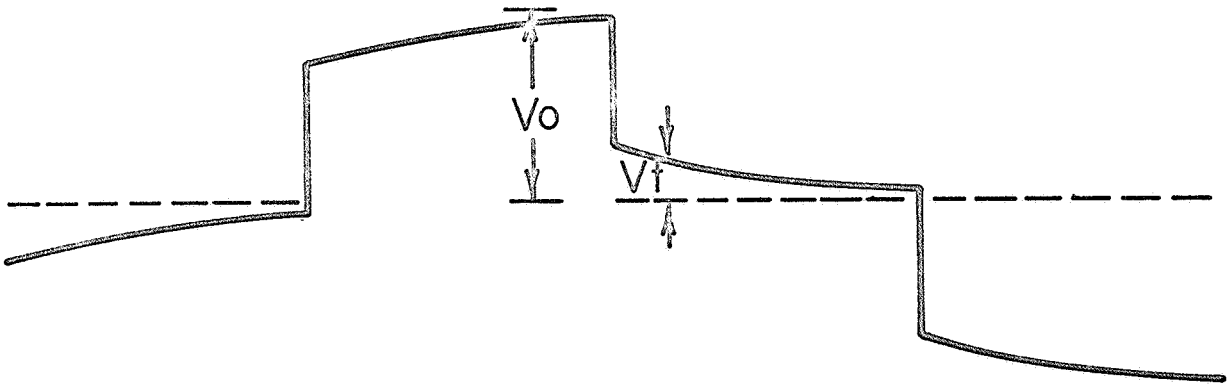

$$M = \frac{1}{V_o} \int V_t \, dt$$

$$= R_{DC} C$$

$$V_t = V_o \left[\frac{R_{DC}}{R_{DC} + R_P} \right] e^{-t/\tau}$$

$$\text{WHERE } \tau = \left(R_P + R_{DC} \right) C$$

INDUCED POLARIZATION IN ROCKS

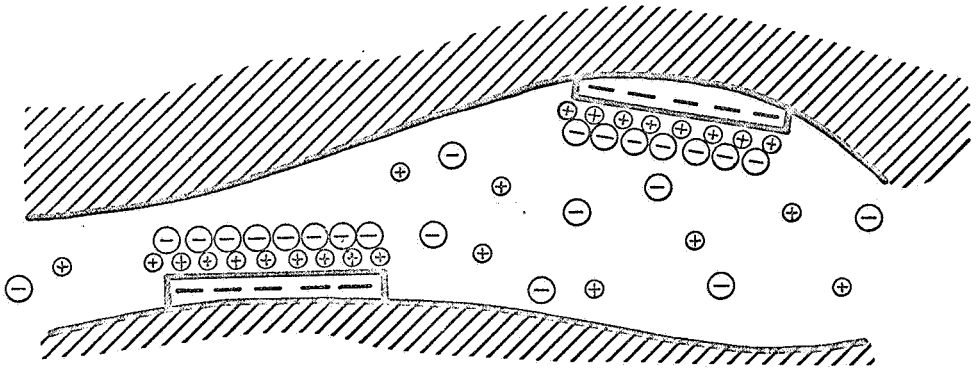

MEMBRANE POLARIZATION

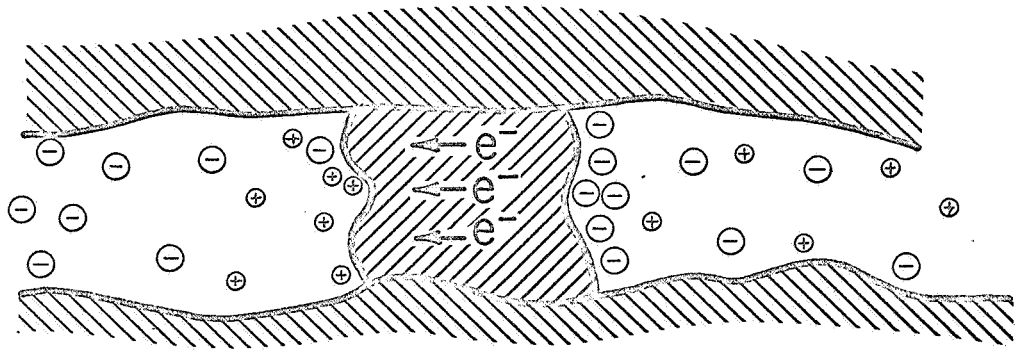

ELECTRODE POLARIZATION

POTENTIALS NEAR A SPHERE IN A PARALLEL ELECTRIC FIELD

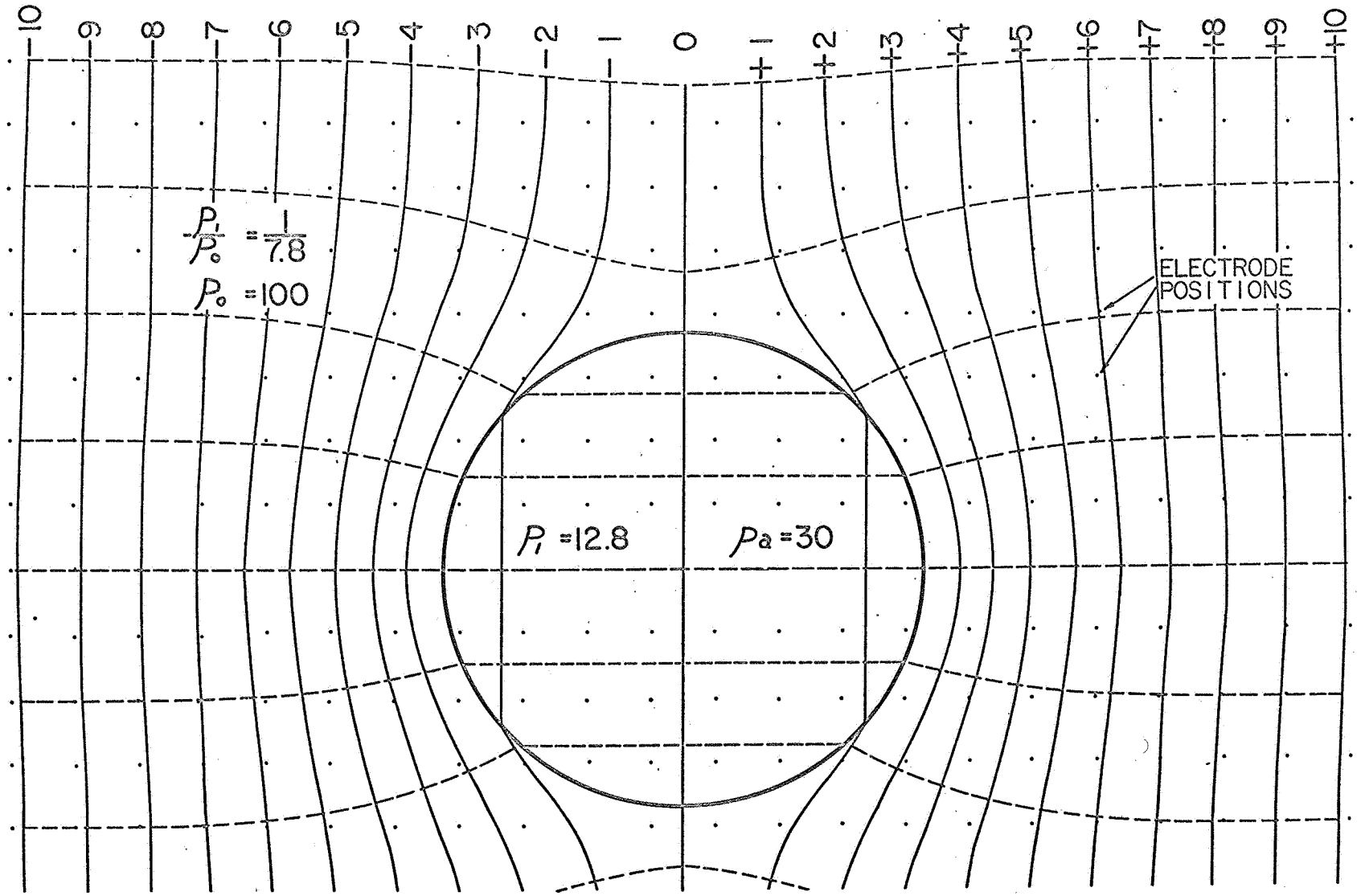

POTENTIAL AND FIELD THROUGH A PLANE POLARIZED SPHERE.

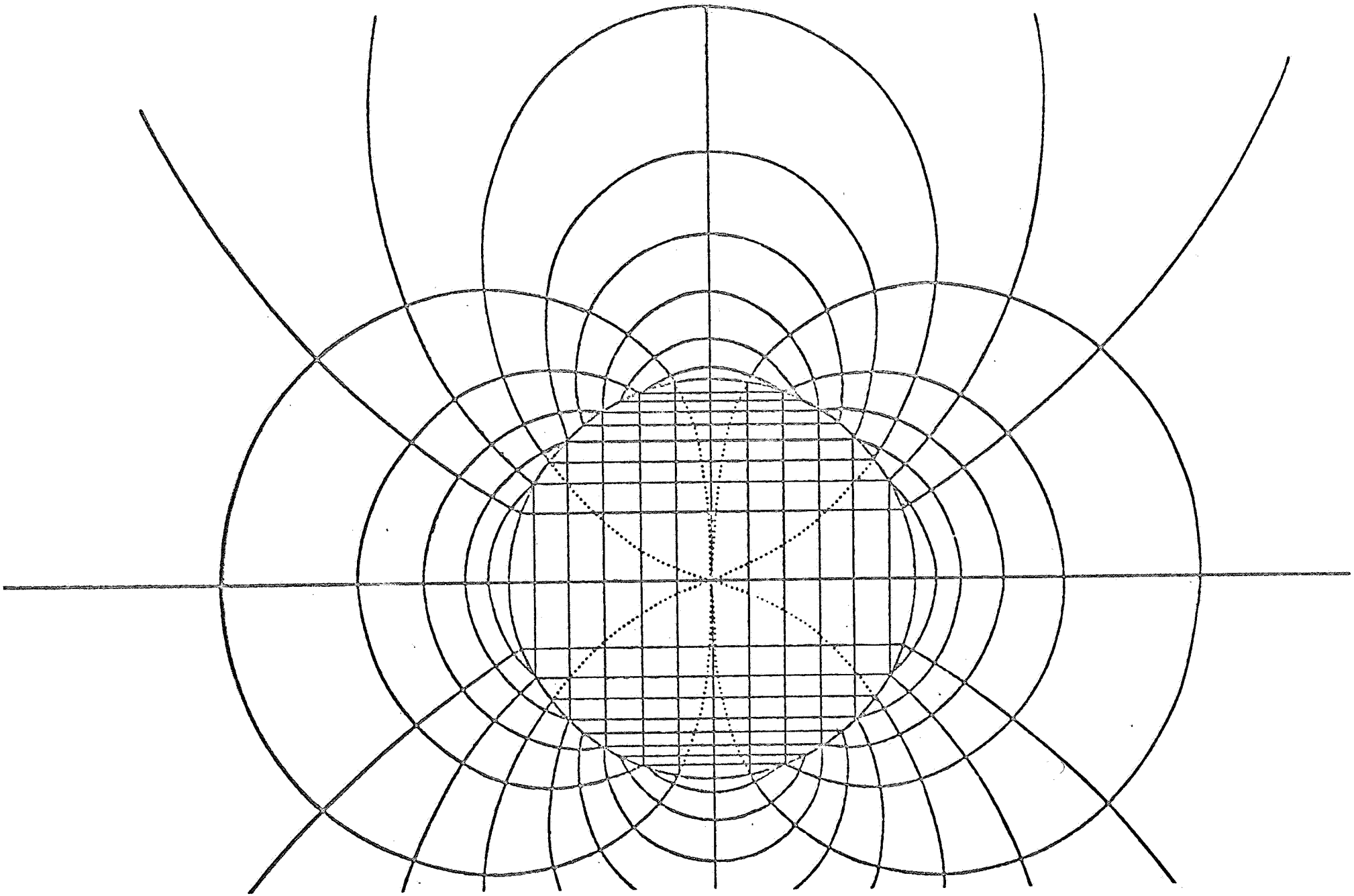

POTENTIAL GRADIENTS NEAR A SPHERE IN A PARALLEL ELECTRIC FIELD

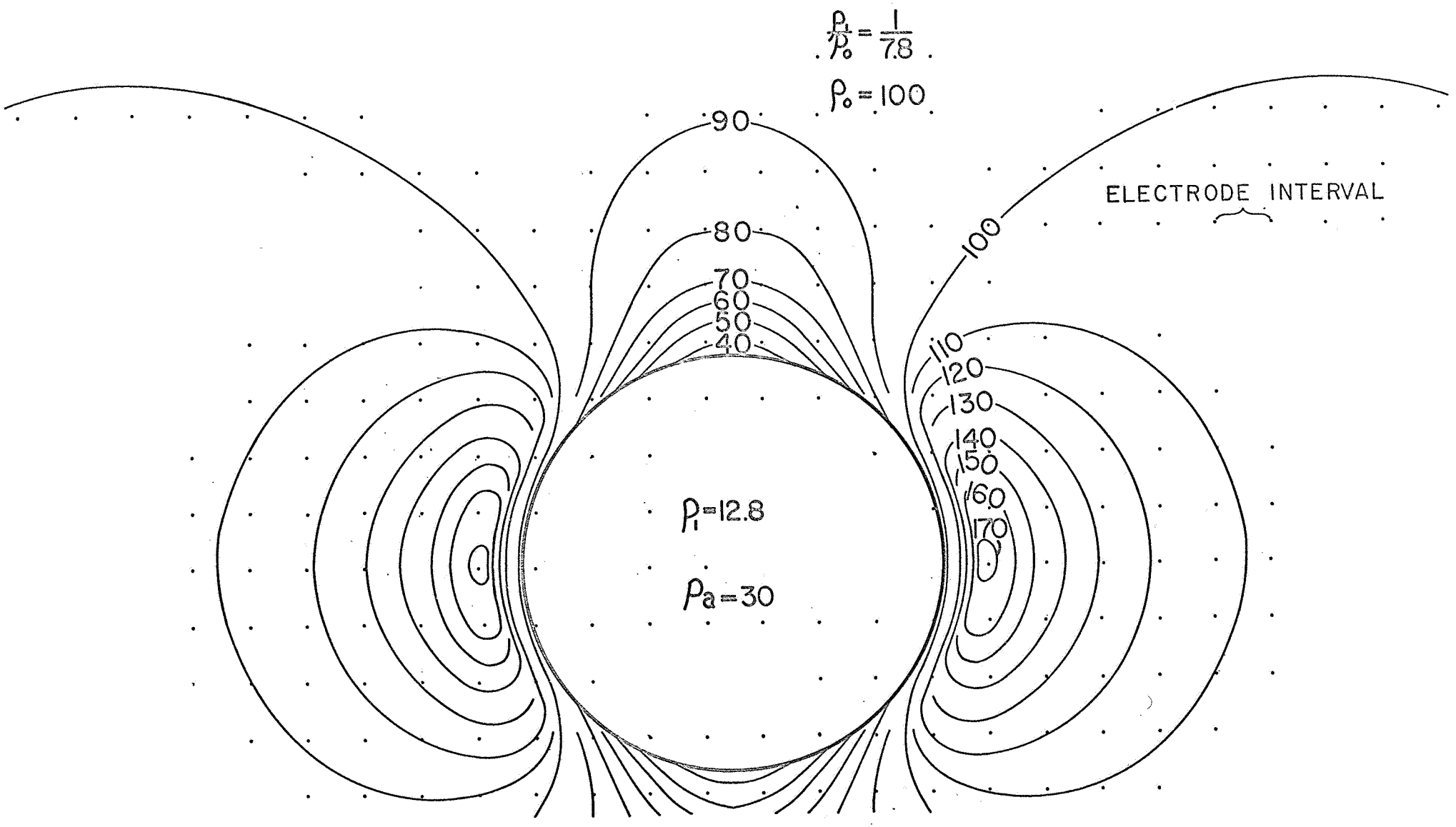

I P VALUES NEAR A SPHERE IN A PARALLEL FIELD

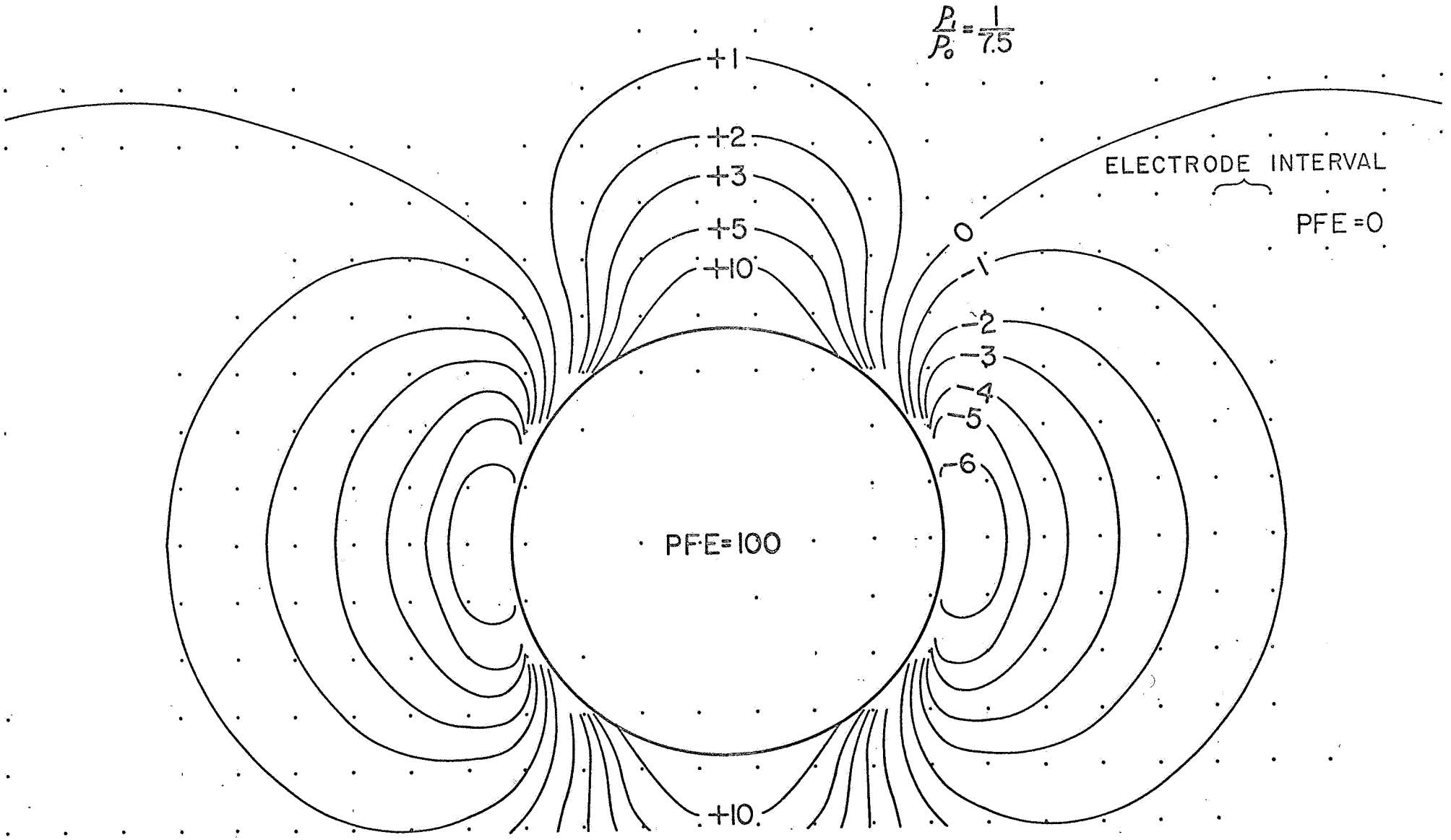

ANALYSIS OF THE POLARIZATION FIELD

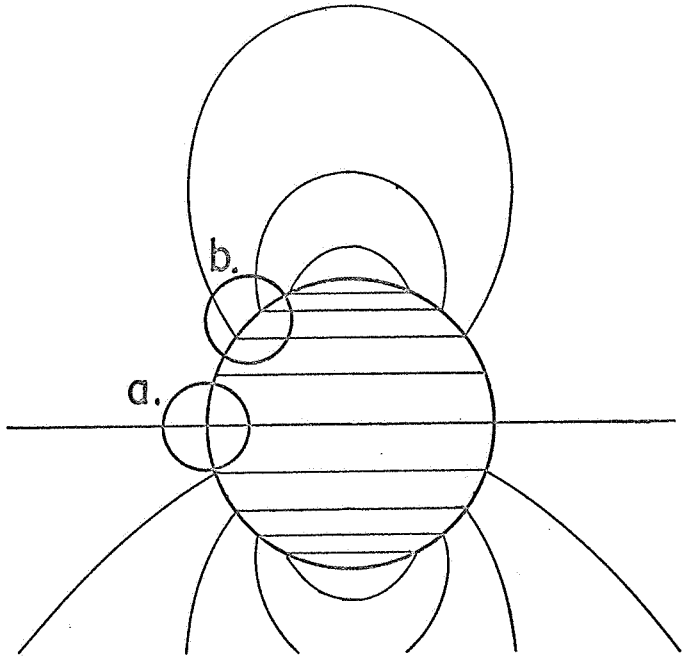

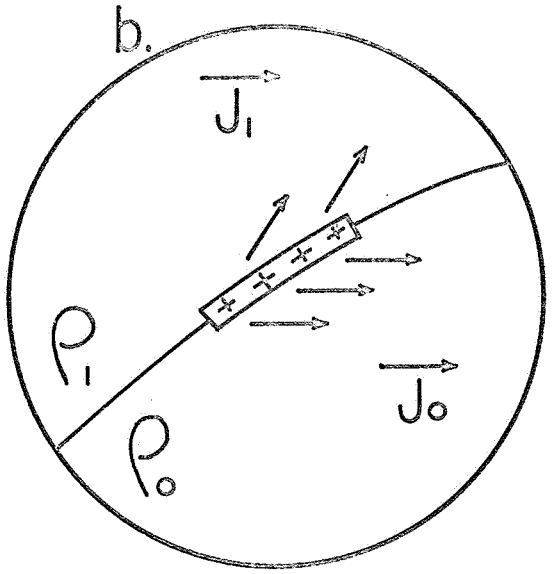

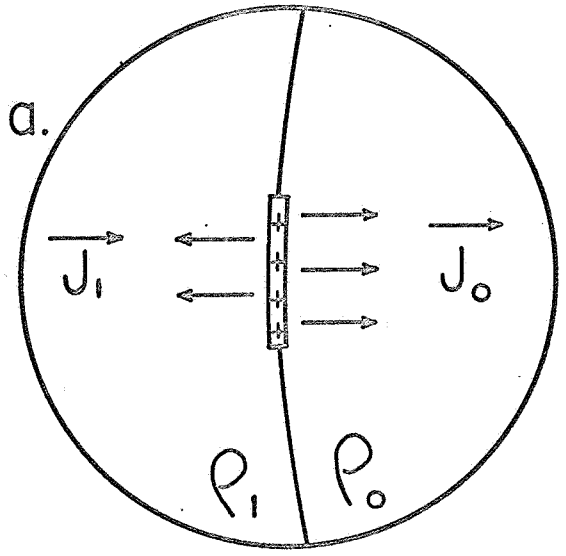

$$\vec{E} = \rho \vec{J}$$

$$-E_{n1} = E_{no}$$

$$\rho \vec{J_{n1}} = \rho_o \vec{J_{no}}$$